Development of a Microscale Cell Culture Analog To Probe Naphthalene Toxicity

Kwanchanok Viravaidya, Aaron Sin, and Michael L. Shuler*

School of Chemical and Biomolecular Engineering, Cornell University, Ithaca, New York 14850-5201

Prediction of human response to drugs or chemicals is difficult as a result of the complexity of living organisms. We describe an in vitro model that can realistically and inexpensively study the adsorption, distribution, metabolism, elimination, and potential toxicity (ADMET) of chemicals. A microscale cell culture analog (μCCA) is a physical replica of the physiologically based pharmacokinetics (PBPK) model. Such a microfabricated device consists of a fluidic network of channels to mimic the circulatory system and chambers containing cultured mammalian cells representing key functions of animal "organ" systems. This paper describes the application of a two-cell system, four-chamber μCCA ("lung"-"liver"-"other tissue"-"fat") device for proof-of-concept study using naphthalene as a model toxicant. Naphthalene is converted into reactive metabolites (i.e., 1,2-naphthalenediol and 1,2-naphthoquinone) in the "liver" compartment, which then circulate to the "lung" depleting glutathione (GSH) in lung cells. Such microfabricated in vitro devices are potential human surrogates for testing chemicals and pharmaceutics for toxicity and efficacy.

Introduction

Accurate prediction of human response to various chemicals and drugs is difficult. For example, most drug candidates fail in human clinical trials as a result of unanticipated toxic side effects. Early prediction of ADMET (adsorption, distribution, metabolism, elimination, and toxicity) can facilitate the drug development process. Similar difficulties exist for evaluating environmental risks due to exposure to various chemicals and chemical mixtures. Currently, the most reliable and widely used model is the animal model. However, there is considerable concern whether animal studies can precisely predict human risk because there is no rational mechanistic basis for extrapolation to low doses and cross species extrapolation is known to be problematic in some cases. Moreover, the use of animals is subject to significant expense, ethical issues, and lengthy experiments. An in vitro model that can realistically and inexpensively test the response of humans and animals to various chemicals is needed.

Here we described an in vitro system that may be able to improve our ability to predict animal and human response to chemical exposure. A cell culture analog (CCA) system is a physical replica of the physiologically based pharmacokinetic (PBPK) model (Figure 1a). This device consists of an array of channels or chambers containing cultured mammalian cells selected to mimic different animal "organ" systems. Design parameters such as "organ" compartment residence times and flow distribution are based on a corresponding PBPK model, and the fluidics is designed to mimic essential features of the circulatory system with recirculating culture medium as a blood surrogate. Unlike other in vitro systems (usually static), a CCA has the potential to mimic the dose dynamics that would occur in an animal or human.

Initial prototype CCA devices have been macroscale (*1*, *2*), but we believe that microscale systems built using the techniques of microfabrication (Figure 1b) would be advantageous. A microscale CCA (μCCA), also called "animal-on-a-chip", may be constructed to better mimic the appropriate physiological scale (e.g., characteristic dimensions of tens of microns). Further microscale systems would allow many tests to be conducted with minimal amount of potentially expensive reagents and of scarce cell or tissue material. Microfabrication technology provides identical units at low cost, facilitating rapid parallel testing. Although we use cell lines to represent "organ compartments" in this proof-of-concept device, we recognize that they are poor mimics of the actual organs. However, tissue-engineered constructs can, in principle, be used in such systems, and those would more closely reproduce the features of organs.

Previously, Sin et al. have described the design, fabrication, and operation of a simple three-chamber μCCA system ("lung"-"liver"-"other tissue") (*3*). The device was fabricated from silicon substrate using standard lithography technique and enclosed between two Plexiglas pieces. Microfluidics was verified and mammalian culture (L2 and H4IIE) viability in the μCCA device was maintained with fluid recirculation for at least 24 h. In addition, a fluorescent-based oxygen sensor was integrated into the system to investigate the adequacy of O_2 transfer in the system operating with cells. Results indicate that O_2 exchange rate is sufficiently rapid to fully meet the need of cells cultured in the μCCA device.

Naphthalene has been chosen as our model toxicant, and the pathway of naphthalene biotransformation is illustrated in Figure 2. Many other polycyclic aromatic hydrocarbon (PAH) compounds undergo similar metabolism. Briefly, naphthalene is metabolized by the cyto-

* To whom correspondence should be addressed. Phone: (607) 255-7577. Fax: (607) 255-9166. Email: mls@cheme.cornell.edu.

10.1021/bp0341996 CCC: $27.50
Published on Web 09/26/2003

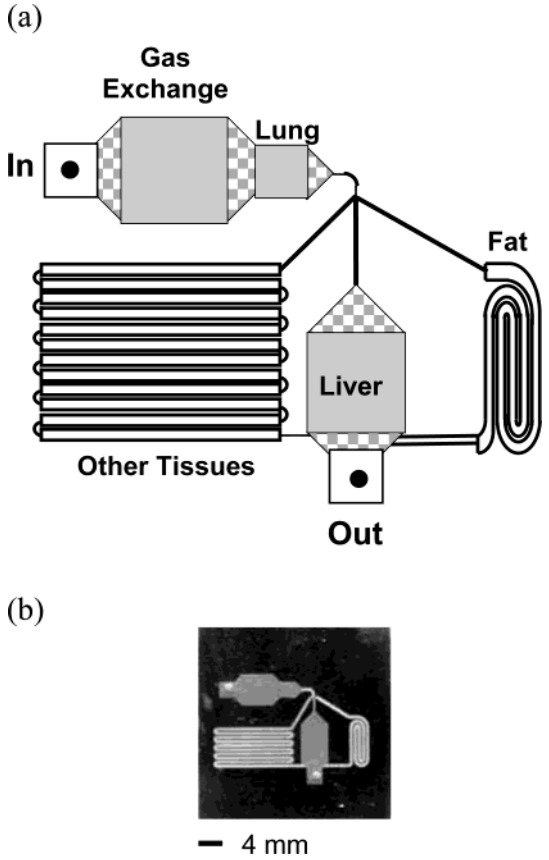

Figure 1. A schematic diagram of 1″ × 1″ μCCA design. Dimensions of each chamber are as followed (w × l × d): lung (2 mm × 2 mm × 20 μm), liver (3.5 mm × 4.6 mm × 20 μm), fat (0.42 mm × 50.6 mm × 100 μm), and other tissues (0.4 mm × 109 mm × 100 μm). Note that, according to the PBPK model, 25%, 9%, and 66% of flow from the lung chamber go to liver, fat, and other tissues chambers, respectively. The fat chamber represents a slowly perfused organ and contains no cells. (b) The actual size of μCCA; the scale bar indicates 4 mm.

chrome P450 monooxygenase system (CYP450) into naphthalene epoxide, which can undergo several competing reactions: conjugation to glutathione (GSH), binding to protein, nonenzymatic rearrangement into naphthol, or enzymatic conversion to dihydrodiol (*4*). Both naphthol and dihydrodiol are enzymatically converted to naphthalenediol (*5*, *6*), which is subsequently oxidized to naphthoquinone through redox cycling, generating reactive oxygen species (ROS) (*7*). These reactive oxygen species may cause severe oxidative stress within the cells, leading to cell death. Naphthoquinone can conjugate with cellular GSH, which reduces ROS formation, and these metabolites can be secreted (*8*). In addition, quinone can form adducts with proteins or DNA (*9*), leading to cellular damage. It has been observed in mice that metabolites generated in the liver can circulate to the lung, causing cell death (*10*).

In this study, we use naphthalene as a model toxicant in proof-of-concept experiments to test the feasibility of constructing a μCCA system. A very simple four-compartment model ("lung"-"liver"-"other tissue"-"fat") model fabricated in silicon is used. Two chambers ("lung" and "liver") contain living cells, whereas the "other tissue" and "fat" compartments have no cells but mimic the distribution of fluid in rapidly and slowly perfused tissues. We test the hypothesis that reactive metabolites generated in the "liver" circulate to cause glutathione depletion and death in the "lung" chamber.

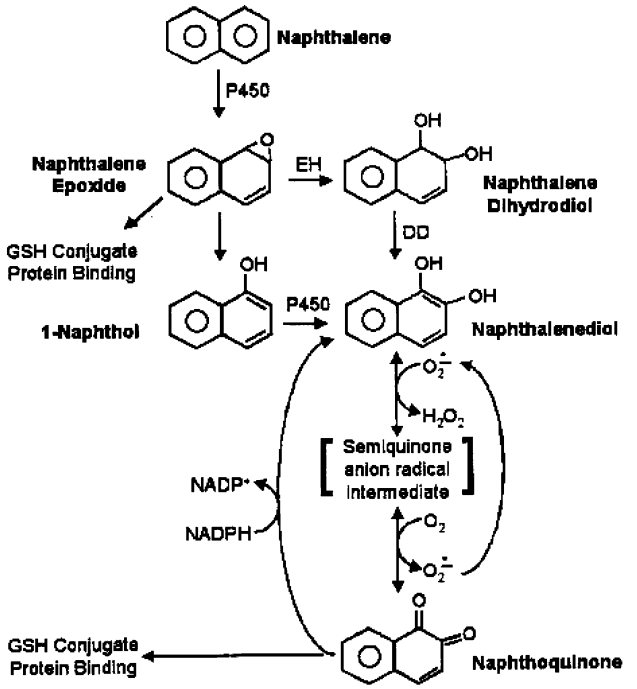

Figure 2. Overview of the naphthalene metabolic pathway. P450 = cytochrome P450 monooxygenase, EH = epoxide hydrolase, DD = dihydrodiol dehydrogenase, GSH = glutathione.

Materials and Methods

Materials. All medium components, unless otherwise indicated, including DMEM/F12 (1:1), fetal bovine serum (FBS), penicillin, streptomycin, pyruvate, and phosphate-buffered saline (PBS) were purchased from Life Technologies, Inc. (Rockville, MD). Other reagents, such as naphthalene, 1-naphthol, 1,2-naphthalene dihydrodiol, 1,2-naphthahlene diol, 1,2-naphthoquinone, poly-D-lysine, and ethoxyresorufin were obtained from Sigma (St. Louis, MO). Matrigel was acquired through Collaborative Biomedical Products (Bedford, MA). Fluorescence stains, such as calcein and monochlorobimane (MCB), and Amplex Red Hydrogen Peroxide assay kit (A-22188) were purchased from molecular Probes (Eugene, OR).

***μ*CCA Microfluidics Study.** Details of the μCCA device fabrication and system assembly are described elsewhere (*3*, *11*). After the μCCA device was assembled, color dye was pumped through using an external peristaltic pump (205S; Watson-Marlow, Wilmington, MA) at 2 μL/min flow rate to visualize fluid flow and leakage in the system. To measure the residence time in each chamber, the liquid source was switched from deionized (DI) water to silicon oil (Sigma, St. Louis, MO). The movement of the oil−water interface through the chambers was observed under a metallurgical microscope (Fisher Scientific, Pittsburgh, PA) and timed with a stopwatch. The measurement was repeated at least 3 times.

Cell Culture. L2 (rat lung Type II epithelial cells), H4IIE (rat hepatocytes), and HepG2/C3A (human hepatocyte) cell lines were obtained from American Type Culture Collection (ATCC, Bethesda, MD) and maintained in DMEM/F12 tissue culture medium, supplemented with 10% FBS, 50 units/mL of penicillin, and 50 μg/mL of streptomycin. Pyruvate was added to medium for HepG2/C3A.

P4501A Activity Measurement. CYP1A activity in H4IIE and HepG2/C3A was measured using the method from Kelly and Sussman (*12*). Briefly, 10 μM ethoxyre-

sorufin in DMEM without phenol red was added into H4IIE and C3A cells and incubated for 1 h at 37 °C. The supernatant was measured fluorimetrically at 530 nm excitation and 590 nm emission. The result was expressed in fold increase in P450 activity per cell basis.

μCCA Toxicity Experiments. The μCCA chip was initially coated with poly-D-lysine at 10 μg/cm^2. A silicone gasket (GRACE-BIO) was applied to the surface of the silicon chip, providing a hydrophobic barrier to confine cell suspensions to the proper compartments and prevent cross contamination of compartments. The lung and liver chambers were then coated with Matrigel at 100 μg/cm^2 density, according to the manufacturer's instructions; 40 μL of L2 at 2×10^5 cells/mL were plated into lung chamber, whereas 40 μL of either HepG2/C3A or H4IIE at 1×10^6 were seeded into liver chamber. The chips were then kept at 37 °C to let the cells attach. After 4 h, the silicone gasket was removed, and DMEM/F12 medium was added to maintain the cells overnight.

The μCCA device was placed between two machined Plexiglas pieces (1/4" thick) and screwed tightly together to ensure no leakage. The chip was then connected to a 100 μL reservoir (debubbler) and a peristaltic pump to provide recirculation at 2 μL/min. DMEM/F12 supplemented with 10% FBS was used as a blood surrogate. The system was operated at 37 °C in a humidified, 5% CO_2 atmosphere. In naphthalene toxicity studies, naphthalene was maintained at the saturation limit. To obtain time course data, multiple experiments were required as the addition of stain terminated that experiment. In naphthoquinone toxicity study, μCCA chips were treated with various concentration of naphthoquinone for 6 h. At the end of each experiment, cells on the chip were stained with calcein (LIVE stain) and monochlorobimane (MCB; GSH stain) (*13*) by recirculating DMEM medium without phenol red containing 5 μM calcein and 80 μM MCB at 37 °C for 30 min.

Fluorescence Microscopy and Image Analysis. Fluorescence images were acquired using an epifluorescence microscope (Metamorph) equipped with 20× objective. Fluorescence from MCB-GSH adduct was excited by light provided by xenon lamp using 10 nm band-pass filter centered at 360 nm in the light path and emitted through a 460 nm long-pass filter, while fluorescent calcein was excited at 483 nm excitation and 535 nm emission. Image analysis to obtain fluorescent intensity used Scion Image (Scion Corporation, Frederick, MD).

Microplate Assay. To study the toxicity of naphthalene metabolites, L2 cells were treated with 0.01 to 20 μg/mL of various naphthalene metabolites for 6 h in 96-well plates (Corning). The toxicity was determined from (1) MTS assay, (2) intracellular GSH, and (3) hydrogen peroxide (H_2O_2) production. L2 cells were plated at 3,000 cells per well for MTS assay and 50,000 cells per well for the experiments that measure intracellular GSH and H_2O_2 production and incubated overnight. These 3 assays were performed independently. The MTS assay measured the cellular metabolic activity and was performed according to standard procedure (*14*).

GSH measurement was determined following protocol from Sebastia et al. (*15*). After L2 cells had been treated with naphthalene metabolites, cells were washed twice to completely remove serum and excess metabolites. Next, 100 μL of 10 μM MCB in DMEM serum-free medium was added to each well and incubated at 37 °C for 1 h, protected from light. The experiment was terminated by removing the MCB solution and replacing with fresh DMEM without phenol red. The fluorescence of the MCB-GSH adduct was immediately observed with excitation at 380 nm and emission at 470 nm. Results were obtained by subtracting blank values and presented as a percentage of control cells not exposed to naphthalene.

Hydrogen peroxide was quantified by using an Amplex Red hydrogen peroxide assay, according to the manufacturer's instruction. Medium was DMEM (without phenol red) serum-free medium. The samples were read for absorbance at 560 nm. To correct for background absorbance, each point value was subtracted from the value of negative control.

Statistics. An unpaired Student's *t*-test was used for data analysis. Significant difference was defined at the 95% confidence level.

Table 1. Comparison between Residence Time Measured from the Chip and Residence Time Used in Calculation; Measurement Was Repeated at Least Three Times

compartment	calculated residence time (s)	measured residence time (s)
lung	2	2
liver	28	38 ± 10
fat	134	120 ± 12
other-tissue	207	200 ± 20

Results

Design and Microfluidics of a Four-Chamber μCCA. A schematic diagram and an actual size four-chamber μCCA are illustrated in Figure 1. The culture medium or blood surrogate first entering the system through the inlet passes through to the "lung", after which 9%, 25%, and 66% of fluid go into the "fat", "liver" and "other tissue" chambers, respectively. The fluid from these three chambers is then combined before being pumped out through the outlet and circulated back to the inlet.

To verify the microfluidics, the residence time measured in each chamber was compared with the actual residence time. According to Table 1, the measured residence time values are fairly close to the design residence time values, although there are some variations in the "liver", "fat", and "other tissue" chambers. This finding also suggests that the μCCA device has achieved the desired passive flow split from the "lung" chamber to other chambers.

Selection of Cell Lines. A rat lung cell line, L2, was used in the lung compartment and was used as a reporter cell line for toxicity (*16*). L2 contains no detectable P450 activity. In our macroscale studies (*1*, *2*), the H4IIE cell line was used as a model for liver because it possesses cytochrome P4501A1 and glutathione-*S*-transferase activity, which are critical enzymes in naphthalene metabolism. Recently, the HepG2/C3A cell line, a subclone of HepG2, has been reported to express high P450 activity (*17*). We compared the P450 activity of H4IIE with that of C3A. Our result indicated that the C3A cell line expressed P4501A activity 30 times higher per cell basis than that of the H4IIE cell line, although the C3A level is still below that in primary cells. In our initial study, we operated the μCCA device with L2 and H4IIE in the lung and liver compartments, respectively, and challenged this system with naphthalene. We did not observe any changes in GSH in either cell type (data not shown). This result is consistent with the findings from Ghanem and Shuler (*2*) and Sin (*11*). The C3A cell line is used to represent the liver compartment in this study. Although we refer to "lung" and "liver" in the following discussion, the reader must recognize that these cell lines are far from authentic representations of such organs.

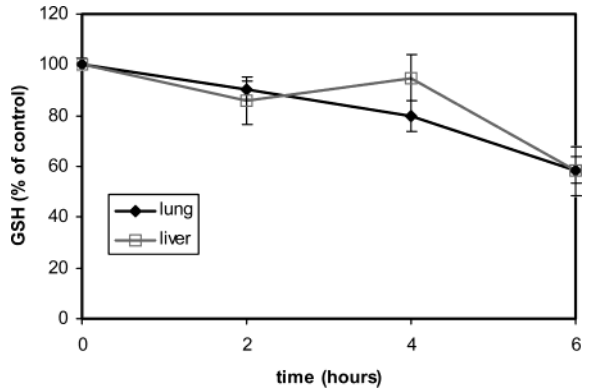

Figure 3. Typical GSH response of L2 (lung) and C3A (liver) cells in μCCA devices after being treated with saturated naphthalene at various time ($n = 3$).

***μ*CCA Naphthalene Toxicity.** Naphthalene concentration was maintained at the saturation level (50 μg/mL in medium supplemented with serum (*11*)); naphthalene's high volatility would lead to significant losses and constantly decreasing concentration. In each experiment, three control μCCA devices were operated in parallel to three naphthalene-treated devices. Afterward, cells were stained with Calcein and MCB. Calcein stain was used as an indicator for viable cells, while MCB stained for GSH.

Calcein stain showed that cells in both compartments, lung and liver, remained attached and viable throughout the experiment (data not shown). Figure 3 presents intracellular GSH, as percentage of controls, of L2 and HepG2/C3A cells after being treated with naphthalene at varying lengths of time. The level of GSH in both naphthalene-treated L2 and C3A cells gradually decreased to about 60% of control cells at 6 h. However, unlike L2 cells, the level of GSH in C3A was slightly higher at 4 h than at 2 and 6 h.

***μ*CCA Control Experiment.** To determine if C3A cells in the liver compartment were responsible for GSH depletion in L2 cells, μCCA devices were operated in the following combinations: (1) L2 in lung and no cell in liver compartment (lung-blank), (2) L2 in both lung and liver compartments (lung-lung), and (3) C3A or (4) H4IIE cells in liver compartment without any cell in lung compartment (blank-liver). GSH status in each combination was compared to GSH in μCCA devices containing L2 in lung and C3A in liver (lung-liver). Results are summarized in Table 2.

After 6 h experiment, there was no intracellular GSH depletion in L2 observed in the L2-blank combination as compared to controls. This result shows that naphthalene by itself does not have any effect on GSH depletion in L2 cells. To test whether metabolizing cells are responsible for depleting GSH as shown in Figure 3, μCCA devices were operated with L2 cells in both lung and liver compartment under the same conditions. GSH level in L2 cells in the lung-lung system was similar to GSH level in the control experiment, indicating that metabolizing cells are required for GSH depletion in L2 cells.

To determine whether C3A cells were affected by circulating metabolites, a blank-liver system was used (no cell in lung compartment). The level of GSH in C3A cells was reduced to about half of that of control cells, which is consistent with the finding from Figure 3, suggesting that naphthalene metabolites do affect the intracellular GSH in C3A cells. When C3A cells were replaced by H4IIE cells, the level of GSH in H4IIE did not vary significantly from control experiment, possibly because H4IIE cells did not have sufficient P450 activity to convert a significant level of naphthalene into toxic metabolites.

Table 2. GSH Level in L2 and C3A in Control Experiment[a]

conditions	lung chamber GSH (% of control)	liver chamber GSH (% of control)
(1) L2-blank	102 ± 7.5	
(2) L2-L2	106 ± 10.5	
(3) blank-C3A		49 ± 10
(4) blank-H4IIE		95 ± 8.5

[a] μCCA system was operated in the following combinations: (1) L2 in both lung and liver chambers, (2) L2 in lung and no cell in liver, (3) C3A in liver and no cell in lung, and (4) H4IIE in liver and no cell in lung chamber ($n = 3$),

Results from Figure 3 and Table 2 strongly support a hypothesis that reactive metabolites generated in the liver compartment are responsible for GSH depletion in both lung and liver cells.

Naphthalene Metabolites Toxicity. To characterize which reactive metabolites of naphthalene are responsible for cytotoxicity in L2, L2 cells were treated with various concentrations of naphthalene metabolites (0.01−20 μg/mL) in static environment for 6 h. According to the naphthalene metabolic pathway (Figure 2), naphthalene is metabolized into many different reactive intermediates. In this study, we focused on the toxicity of four metabolites: 1-naphthol, 1,2-dihydro naphthalene 1,2-diol (naphthalene dihydrodiol), 1,2-naphthalene diol, and 1,2-naphthoquinone.

MTS Assay. Toxicity of naphthalene metabolites was assessed using a colorimetric MTS assay (Figure 4a). MTS tetrazolium compound is bioreduced by metabolically active cells into a colored formazan product, which can be related to the metabolic state of the cells and cell viability (*18*). Result was expressed in percentage of cell viability in treated cells to that of untreated cells. As shown in Figure 4a, 1-naphthol and naphthalene dihydrodiol isomers did not affect the viability of L2 cells even at high concentration (20 μg/mL) where cell viability remained at about 90−98%. On the other hand, both naphthalene diol and naphthoquinone significantly decreased cell viability ($p < 0.0001$) in a concentration-dependent manner. Naphthoquinone is shown to be more toxic toward L2 than naphthalene diol, as the EC_{50} of naphthoquinone (1.5 μg/mL) was much less than that of naphthalene diol (10 μg/mL). Nonetheless, L2 cells remained unaffected by these metabolites up to a concentration of 0.5 μg/mL. L2 cells were also treated with 1:1 ratio mixture of naphthalene diol and naphthoquinone. The mixture was less toxic than naphthoquinone but more toxic than naphthalene diol, which implied that there was no synergistic effect between reactive metabolites.

GSH Determination. We also investigated the effect of naphthalene metabolites on GSH depletion in L2 cells (Figure 4b). L2 cells were treated under the same condition as in the MTS assay. Naphthol and naphthalene dihydrodiol did not significantly alter intracellular GSH, as GSH level remained high throughout the experiment. However, both naphthalene diol and naphthoquinone significantly decreased GSH ($p < 0.001$), although GSH level did not vary significantly at lower concentration of both metabolites (0.01−0.5 μg/mL). GSH depletion was also concentration-dependent, and naphthoquinone was more potent in GSH reduction as compared to naphthalene diol. Interestingly, 2.5 and 5 μg/mL of naphthalene diol increased GSH level in L2. In

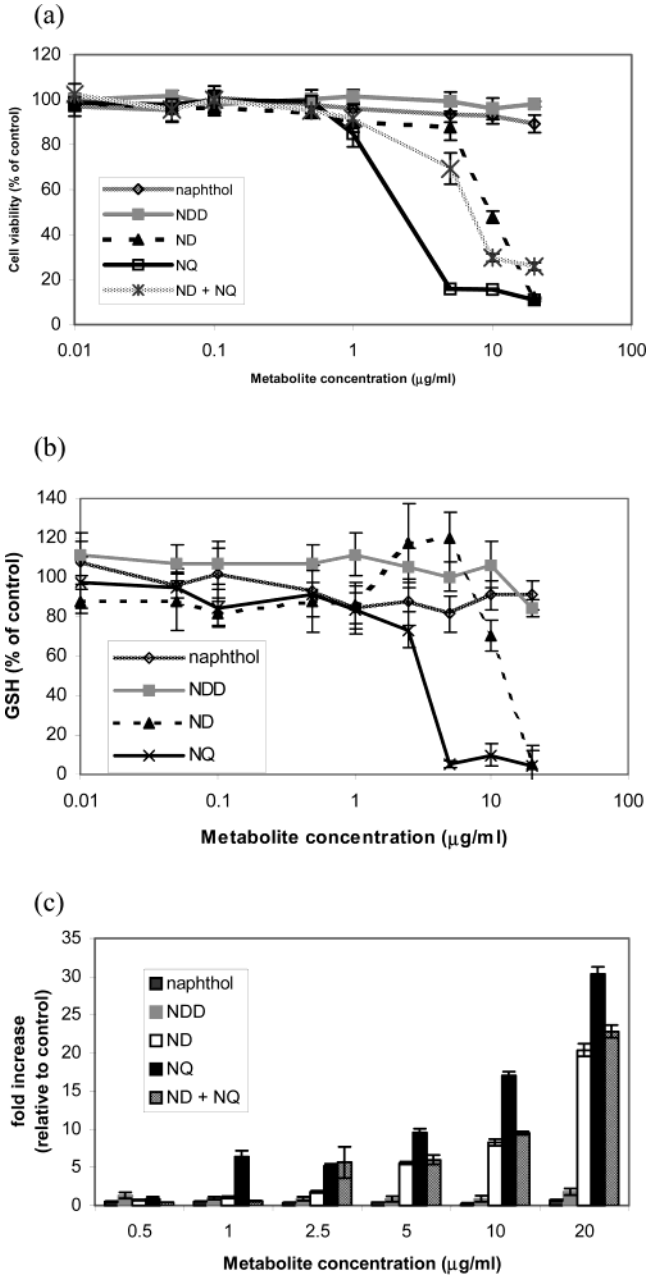

Figure 4. L2 cells were treated with various concentrations of naphthalene metabolites (naphthol, naphthalene dihydrodiol, naphthalene diol, and naphthoquinone) for 6 h. The cytotoxicity of these metabolites was determined based on (a) MTS assay, (b) intracellular GSH, and (c) H_2O_2 production. NDD, ND, and NQ indicate naphthalene dihydrodiol, naphthalene diol, and naphthoquinone, respectively ($n = 6$).

general, GSH depletion profiles of all four naphthalene metabolites matched well with cytotoxicity profiles obtained from MTS assay. These results demonstrated that naphthoquinone was more cytotoxic toward L2 cells than naphthalene diol, whereas naphthol and naphthalene dihydrodiol were not cytotoxic to this cell line.

H_2O_2 Production. To further confirm the mechanism of naphthalene toxicity, H_2O_2 formation in L2 cells treated with various naphthalene metabolites was measured as an indicator of redox cycling and oxidative stress. This experiment was carried out in serum-free DMEM medium without phenol red because phenol red and serum protein interfered with fluorescence detection. According to Figure 4c, only naphthalene diol and naphthoquinone accumulated H_2O_2 in a concentration-dependent manner. At the same concentration, the amount of H_2O_2 was highest in cells treated with naphthoquinone. This evidence suggests that naphthalene diol and naphthoquinone, but not naphthol and naphthalene dihydodiol, undergo redox cycling in L2 cells.

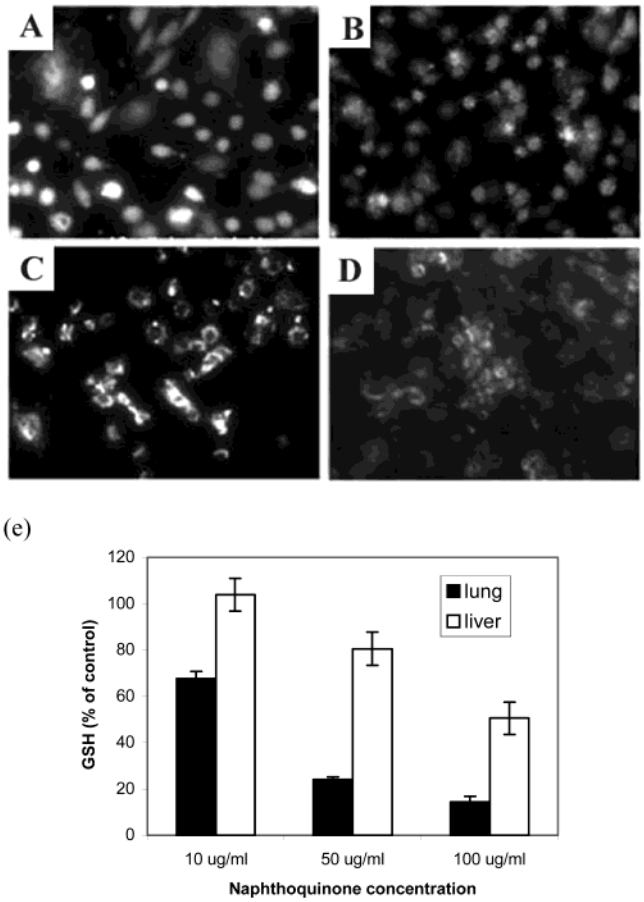

Figure 5. Comparison of the morphology of (a) untreated L2 cells with L2 cells treated with (b) 10, (c) 50, and (d) 100 μg/mL of naphthoquinone for 6 h in μCCA devices. Cells were stained with calcein (×20). In addition, (e) the GSH level in L2 (lung) and C3A (liver) was determined at the end of the experiment ($n = 3$).

***μ*CCA Naphthoquinone Toxicity.** We challenged the μCCA system with 10, 50, and 100 μg/mL of naphthoquinone for 6 h, using the same experimental apparatus as in the naphthalene toxicity study. Calcein stain revealed that naphthoquinone drastically changed the morphology of L2 cells from fibroblast-like (Figure 5a) to more rounded structure (Figure 5b−d). This effect was more pronounced at high concentration. Interestingly, calcein was unevenly distributed in L2 cultures treated with 50 and 100 μg/mL naphthoquinone. Unlike L2 cells, the morphology of C3A did not change upon being exposed to naphthoquinone (data not shown).

GSH in both cell lines, L2 and C3A, decreased with increasing concentration of naphthoquinone (Figure 5e). However, L2 cells were more sensitive than C3A, as the level of GSH in L2 was much less than that of C3A treated at the same concentration of naphthoquinone.

GSH Depletion by Naphthoquinone. To investigate the different responses between L2 and C3A cell lines on GSH depletion causing by naphthoquinone, both cells were incubated with various concentrations of naphthoquinone for up to 6 h. This study was carried out in a 96-well tissue culture plate. At the end of the experiment, GSH level in both cell types was measured on the basis of fluorescence intensity of GSH-MCB adduct. As shown

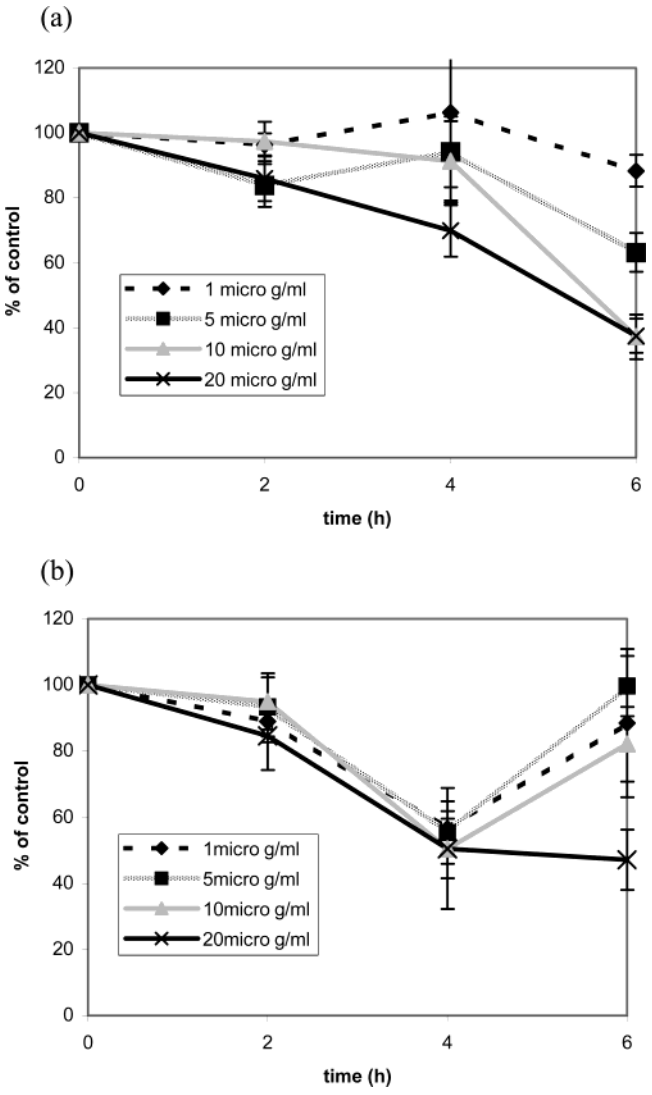

Figure 6. GSH responses of (a) L2 cells and (b) HepG2/C3A cells upon incubation with various concentrations of naphthoquinone for up to 6 h ($n = 6$).

in Figure 6a, GSH level in L2 cells decreased in a concentration- and time-dependent manner. On the other hand, the level of GSH in C3A cells reached the minimum at 4 h and then, except for naphthoquinone at 20 μg/mL, increased to about 80−100% of GSH in control cells (Figure 6b). This result suggests a significant level of GSH resynthesis in C3A cells after 4 h. The GSH resynthesis in C3A cells exposed to the highest concentration of naphthoquinone (20 μg/mL) is not adequate to replenish the depleted GSH within the cells. Overall, GSH resynthesis rate of C3A is faster than that of L2 cells.

Discussion

The "fat" compartment is added to the previous three-chamber μCCA system to better mimic the fluid distribution in rapidly and slowly perfused organs and more accurately predict the response of animals to chemicals. To validate the microfluidics, the residence time in each chamber was measured and compared to the actual residence time (Table 1). These residence times matched reasonably well, confirming the correct fluid distribution into the "liver", "fat", and "other tissue chamber". The fluid flow is passively controlled by channel geometry that also determines the resistance of the fluid channel (*19*). By balancing the fluid resistance between the "liver", "fat", and "other tissue" chambers, pressure required to introduce fluid into these particular chambers is similar and therefore the desired fluid distribution is achieved. However, variation in residence time in the "liver", "fat", and "other tissue" was observed, possibly from pulsation in the external peristaltic pump. Although this peristaltic pump can handle μL/min flow rate, it is difficult to use macroscopic equipment to control microscopically. To overcome this limitation, a micropump will be integrated into the future μCCA device. A diaphragm micropump has been developed and is capable of producing recirculation flow and precisely controlling the flow rate as low as 2 μL/min (*20*). In addition, the nonphysiologically realistic external residence time outside the μCCA chip due to the debubbler will be significantly reduced.

A key feature of μCCA device is the dynamic co-culture system that allows us to address different roles of metabolizing cells (HepG2/C3A) and nonmetabolizing cells (L2) in naphthalene toxicity. The primary biomarker for toxicity in this study is glutathione depletion. Our results demonstrate that reactive metabolites produced by HepG2/C3A cells in the liver compartment circulate to lung compartment and decrease GSH level in L2 cells in a time-dependent manner. C3A cells were also affected by naphthalene metabolites. Although the metabolites were not directly measured in this system, results from naphthalene and control experiments indicate the formation of metabolites in liver cells that then circulated to the "lung" compartment, altering L2 GSH. According to the lung-lung and lung-blank controls, naphthalene is not cytotoxic and the presence of P450 enzyme is necessary for naphthalene-induced GSH depletion, which is consistent with the accepted understanding of naphthalene toxicity. Also, the C3A cell line is superior to the H4IIE cell line in mimicking liver metabolism, as a result of higher P450 enzyme activity. Note that H4IIE cells were not capable of metabolizing naphthalene at significant rates, as there was no reduction in GSH level observed in either L2 or H4IIE when H4IIE cells were cultured in liver compartment.

These responses in the μCCA are consistent with observations from the macroscopic CCA systems (lung-liver-other tissues) and the corresponding PBPKs (*1*, *2*, *4*). In those systems toxicity was related to P4501A1 activity and whether the design allowed for significant formation of 1-naphthol. Although early animal studies on naphthalene metabolism suggested that the naphthalene epoxides were the toxic agents (*21*, *22*), the CCA models and more recent experiments (*5*, *23*−*26*) all suggest that toxicity is related to quinone formation. With the μCCA system used here, naphthalene epoxides could not be active agents. The half-life of naphthalene epoxide is 3.6 min in aqueous medium (*27*) because of relatively rapid rearrangement into 1-naphthol. Since the liquid residence time in the debubbler unit was large (50 min), very little of the naphthalene epoxide (less than 0.007%) formed in the HepG2/C3A line would have been returned to the lung.

Our results indicate that up to 20 μg/mL of either naphthol or naphthalene dihydrodiol did not alter cell viability or GSH level in L2 cells. On the other hand, naphthalene diol and naphthoquinone significantly decreased cell viability and depleted GSH in a concentration-dependent manner. In addition, naphthoquinone was the most toxic toward L2 cells among all metabolites tested and there was no synergistic interaction between naphthalene diol and naphthoquinone (Figure 4a and c). Only quinone has the potential to form thiol conjugates

with cellular nucleophiles, such as GSH, DNA, and protein, leading to cellular damage (*28*, *29*). Naphthalene diol likely depleted GSH in L2 cells by reacting to form quinone through the redox cycle, which then conjugated with GSH. Previous studies have suggested that naphthalene can also induce oxidative stress in experimental animals (*30*, *31*). Only naphthalene diol and naphthoquinone were capable of generating H_2O_2, which confirms that a redox cycling mechanism exists in this in vitro model. In addition, the cytotoxic effects were related to their ability to produce H_2O_2, as H_2O_2 accumulation has been previously shown to induce cell death by changing cellular redox state (*24*, *32*). These observations suggest naphthalene diol and naphthoquinone are the circulating metabolites responsible for GSH depletion of L2 cells in μCCA device.This suggestion is strengthened by direct addition of naphthoquinone to the μCCA. L2 cells were more susceptible to cellular damage than C3A cells when μCCA devices were treated with various concentrations of naphthoquinone. Naphthoquinone not only reduced GSH level but also caused morphological changes in L2 cells possibly from lipid peroxidation, a common sign of oxidative stress (*33*). These changes were not observed in C3A cells, and reduction in GSH was not to the same extent. Thus, naphthoquinone toxicity is cell type specific. The lung cells are more sensitive to toxicity compared to the hepatoma cells, possibly because of slower GSH resynthesis rate (*34*, *35*), as also shown in Figure 6.

In naphthalene toxicity experiments (Figure 3), we found that the GSH level in L2 and C3A decreased to about the same level (~60% of control), whereas in naphthoquinone toxicity experiments (Figure 5), the GSH level in L2 cells was significantly less than in C3A cells. This evidence shows that naphthoquione and naphthalene diol may not be the only two metabolites affecting the level of GSH in liver cells. Naphthalene epoxide has been shown to conjugate with protein and GSH in cells expressing cytochrome P4501A1 (*5*, *36*). Even though naphthalene epoxide is relatively unstable, it can conjugate with GSH within liver cells in situ as naphthalene was metabolized intracellularly. This effect is, however, not relevant for the GSH depleting effect in lung cells because of long circulation time from liver to lung chamber.

Although the μCCA described here provides a useful framework to probe naphthalene toxicity mechanisms and is satisfactory for proof-of-concept experiments, it has many limitations. Most importantly is that isolated cell lines are not authentic mimics of true organs. This limitation plagues all in vitro systems. However, the μCCA system can be easily redesigned to accommodate tissue engineered constructs employing mixed populations of cells that show more metabolically authentic behavior. Tissue engineering is an area of intense research, and such constructs are in development.

Another limitation is that this μCCA was designed to mimic a rat with respect to ratio of one cell type to another and fluid residence time in each organ; however, the addition of a "debubbler" add a large volume that rendered the circulation dynamics unrealistic. A "debubbler" was necessary to obtain reliable fluid recirculation (*3*, *11*).

Further, a two-cell-type model is of limited utility. However, the design and use of models with many more compartments are straightforward. We have cultured differentiated adipocytes in the fat chamber to simulate the bioaccumulation of tested compounds and anticipated that the presence of fat tissue will modify the dynamic response because of the absorption. In addition, the future μCCA design will incoporate the debubbler as part of the "other tissues" compartment to obtain more realistic distribution of metabolites.

Conclusions

This study demonstrates that the μCCA or "animal-on-a-chip" system provides a useful in vitro model to probe naphthalene metabolism. A four-chamber ("lung"-"liver"-"fat"-"other tissue") μCCA contains culture L2 cells in the "lung" as target organ and HepG2/C3A or H4IIE cells in the "liver" as metabolizing organ. Our results indicate that naphthalene is metabolized by "liver" into reactive metabolites, which then circulate to the "lung", causing GSH depletion in L2 cells. Naphthalene-induced toxicity strongly depends on cytochrome P4501A1 enzyme activity. 1,2-Naphthalenediol and 1,2-naphthoquinone are identified as the circulating reactive metabolites responsible for GSH depletion in L2 cells. In addition, L2 cells are more sensitive toward naphthoquinone than HepG2/C3A, possibly because of slower GSH resynthesis.

These studies verify the potential of a very simple μCCA system to provide mechanistic insight into chemical toxicity. A more complete μCCA system can be readily fabricated to provide in vitro ADMET studies on new drugs or drug combination.

Acknowledgment

This work was supported by the Nanobiotechnology Center (NBTC), a STC Program of the National Science Foundation under Agreement ECS-9876771, the Cornell Center for Advanced Technology (Biotechnology) with support from New York State Science and Technology Foundation and a consortium of industries, as well as a matching gift from DuPont, and support from the Faculty Development Program of New York Science, Technology and Academic Research (NYSTAR). This work was performed in part at the Cornell Nanofabrication Facility (a member of the National Nanofabrication Users Network). We would like to thank Greg Baxter and professor Bill Shain for helpful discussions and Paula Miller and Glenn Swan for their technical assistance.

References and Notes

(1) Sweeney, L. M.; Shuler, M. L.; Babish, J. G.; Ghanem, A. A cell culture analog of rodent physiology: Application to naphthalene toxicology. *Toxicol. In Vitro* **1995**, *9*, 307−316.

(2) Ghanem, A.; Shuler, M. L. Combining cell culture analog reactor designs and PBPK models to probe mechanisms of naphthalene toxicity. *Biotechnol. Prog.* **2000**, *16*, 334−345.

(3) Sin, A.; Chin, K. C.; Jamil, M. F.; Kostov, Y.; Rao, G.; Shuler, M. L. The design and fabrication of three-chamber microscale cell culture analog devices with integrated dissolved oxygen sensor. *Biotechnol. Prog.* (in press).

(4) Quick, D. J.; Shuler, M. L. Use of in vitro data for construction of a physiologically based pharmacokinetic model for naphthalene in rats and mice to probe species differences. *Biotechnol. Prog.* **1999**, *14*, 540−555.

(5) Zheng, J.; Cho M.; Jones, A. D.; Hammock B. D. Evidence of quinone metabolites of naphthalene covalently bound to sulfur nucleophiles of proteins of murine clara cells after exposure to naphthalene. *Chem. Res. Toxicol.* **1997**, *10*, 1008−1014.

(6) Flowers-Geary, L.; Harvey, R. G.; Penning, T. M. Cytotoxicity of polycyclic aromatic hydrocarbon *o*-quinones in rat and human hepatoma cells. *Chem. Res. Toxicol.* **1993**, *6*, 252−260.

(7) Bolton, J. L.; Trush, M. A.; Penning, T. M.; Dryhurst, G.; Monks, T. J. Role of quinone in toxicology. *Chem. Res. Toxicol.* **2000**, *13*, 135−160.

(8) Akerboom, T. M.; Sies, H. Transport of glutathione, glutathione disulfide, and glutathione conjugates across hepatocyte plasma membrane. *Methods Enzymol.* **1989**, *134*, 523−534.
(9) Levay, G.; Pongracz, K.; Bodell, W. J. Detection of DNA adducts in HL-60 cells treated with hydroquinone and *p*-benzoquinone by ^{32}P-postlabeling. *Carcinogenesis* **1991**, *12*, 1181−1186.
(10) Tsuruda, L. S.; Lame, M. W.; Jones, A. D. Formation of epoxide and quinone protein adducts in B6C3F1 mice treated with naphthalene, sulfate conjugate of 1,4-dihydroxynaphthalene and 1,4-naphthoquinone. *Arch. Toxicol.* **1995**, *69(6)*, 362−367.
(11) Sin, A. Development of a three-chamber microscale cell culture analogue device. Ph.D. Thesis, Cornell University, Ithaca, NY, August 2002.
(12) Kelly, J. H.; Sussman, N. L. A fluorescent cell-based assay for cytochrome P-450 isozyme 1A2 induction and inhibition. *J. Biomol. Screen* **2000**, *5* (4), 249−254.
(13) Keelan, J.; Allen, N. J.; Antcliffe, D.; Pal, S.; Duchen, M. R. Quantitative imaging of glutathione in hippocampal neurons and glia in culture using monochlorobimane. *J. Neurosci. Res.* **2001**, *66*, 873−884.
(14) Wong, J. K.; Kennedy, P. R.; Belcher, S. M. Simplified serum- and steroid-free culture conditions for high-throughput viability analysis of primary cultures of cerebellar granule neurons. *J. Neurosci. Methods* **2001**, *110* (1−2), 45−55.
(15) Sebastia, J.; Cristofol, R.; Martin, M.; Rodríguez-Farre, E.; Sanfeliu, C. Evaluation of fluorescent dyes for measuring intracellular glutathione content in primary cultures of human neurons and neuroblastoma SH-SY5Y. *Cytometry* **2003**, *51A* (1), 16−25.
(16) Hopkinson, D.; Bourne, R.; Barile, F. A. In vitro cytotoxicity testing: 24- and 72-hour studies with cultured lung cells. *ATLA* **1993**, *21*, 167−172.
(17) Burke, M. D.; Thompson, S.; Weaver, R. J.; Wolf, C. R.; Mayer, R. T. Cytochrome P450 specificities of alkoxyresorufin O-dealkylation in human and rat liver. *Biochem. Pharmacol.* **1994**, *48*, 923−936.
(18) Chan, F. L.; Choi, H. L.; Chen, Z. Y.; Chan, P. S. F.; Huang, Y. Induction of apoptosis in prostate cancer cell lines by a flavonoid, baicalin. *Cancer Lett.* **2000**, *160* (2), 219−228.
(19) Ahn, C.; Puntambekar, A.; Lee, S.; Cho, H.; Hong, C. Structurally programmable microfluidic systems. In *Micro Total Analysis Systems*; Van den Berg, A., Olthuis, W., Bergveld, P., Eds.; Kluwer Academic: Dordrecht, 2000; pp 205−208.
(20) Sin, A.; Reardon, C. F.; Shuler, M. L. A self-priming microfluidic diaphragm pump capable of recirculation fabricated by combining soft lithography and traditional machining. *Biotechnol. Bioeng.* In press.
(21) Richieri, P. R.; Buckpitt, A. R. Glutathione depletion by naphthalene in isolated hepatocytes and by naphthalene oxide in vivo. *Biochem. Pharmacol.* **1988**, *37* (12), 2473−2478.
(22) Buckpitt, et al. Relationship of cytochrome P450 activity to Clara cell cytotoxicity. IV. Metabolism of naphthalene and naphthalene oxide in microdissected airways from mice, rats, and hamsters. *Mol. Pharmacol.* **1995**, *47(1)*, 74−81.
(23) Wilson, A. S.; Davis, C. D.; Williams, D. P.; Buckpitt, A. R.; Pirmohamed, M.; Park, B. K. Characterisation of toxic metabolite(s) of naphthalene. *Toxicology* **1996**, *114*, 233−242.
(24) Flowers-Geary, L.; Blecziinksi, W.; Harvey, R. G.; Penning, T. M. Cytotoxicity and mutagenicity of polycyclic aromatic hydrocarbon o-quinones produced by dihydrodiol dehydrogenase. *Chem.-Biol. Interact.* **1996**, *99*, 55−72.
(25) Kilanowicz, A.; Czerski, B.; Sapota, A. The disposition and metabolism of naphthalene in rats. *Int. J. Occup. Med. Environ. Health* **1999**, *12* (3), 209−219.
(26) Palackal, N. T.; Burczynski, M. E.; Harvey, R. G.; Penning, T. M. The ubiquitous aldehyde reductase (AKR1A1) oxidizes proximate carcinogen *trans*-dihydrodiols to *o*-quinones: potential role in polycyclic aromatic hydrocarbon activation. *Biochemistry* **2001**, *40*, 10901−10910.
(27) Bounarati, M.; Morin, D.; Plopper, C.; Buckpitt, A. Glutathione depletion and cytotoxicity by naphthalene 1,2-oxide in isolated hepatocytes. *Chem.-Biol. Interact.* **1989**, *71*, 147−165.
(28) Murty, V.; Penning, T. Polycyclic aromatic hydrocarbon (PAH) ortho-quinone conjugate chemistry: Kinetics of thiol addition to PAH ortho-quinones and structures of thioether adducts of naphthalene 1,2-dione. *Chem.-Biol. Interact.* **1992**, *84*, 169−188.
(29) Bolton, J. L.; Trush, M. A.; Penning, T. M.; Dryhurst, G.; Monks, T. J. Role of quinones in toxicology. *Chem. Res. Toxicol.* **2000**, *13* (3), 135−160.
(30) Vuchetich, P. J.; Bagchi, M.; Bagchi, E.; Tang, H. L.; Stohs, S. J. Naphthalene-induced oxidative stress in rats and the protective effects of vitamin E succinate. *Free Radical Biol. Med.* **1996**, *21* (5), 577−590.
(31) Germansky, M.; Jamall, S. Organ-specific effects of naphthalene on tissue peroxidation, glutathione peroxidases, and superoxide dismutase in the rat. *Arch. Toxicol.* **1988**, *61*, 480−483.
(32) Penning, T. M.; Ohnishi, T.; Ohnishi, T.; Harvey, R. G. Generation of reactive oxygen species during the enzymatic oxidation of polycyclic aromatic hydrocarbon trans-dihydrodiols catalyzed by dihydrodiol dehydrogenase. *Chem. Res. Toxicol.* **1996**, *9*, 84−92.
(33) Bagchi, M.; Bagchi, D.; Balmoori, J.; Ye, X.; Stohs, S. J. Naphthalene-induced oxidative stress and DNA damage in cultured macrophage J7741A.1 cells. *Free Radical Biol. Med.* **1998**, *25* (2), 137−143.
(34) D'Souza, R. W.; Francis, W. R.; Andersen, M. E. Physiological model for tissue glutathione depletion and increased resynthesis after ethylene dichloride exposure. *J. Pharmacol. Exp. Ther.* **1988**, *245*, 563−568.
(35) Liu, R.-M.; Choi, J. Age-associated decline in γ-glutamylcystein synthetase gene expression in rats. *Free Radical Biol. Med.* **2000**, *28* (4), 566−574.
(36) Greene, J. F.; Zheng, J.; Grant, D. F.; Hammock, B. D. Cytotoxicity of 1,2-epoxynaphthalene is correlated with protein binding and in situ glutathione depletion in cytochrome P4501A1 expressing Sf-21 cells. *Toxicol. Sci.* **2000**, *53*, 352−360.

Accepted for publication August 25, 2003.

BP0341996